International Journal of Nanoscience
Vol. 17, No. 5 (2018) 1850002 (12 pages)

DOI: 10.1142/S0219581X18500023

Adsorptive Removal of Methylene Blue Using Magnetic Biochar Derived from Agricultural Waste Biomass: Equilibrium, Isotherm, Kinetic Study

M. Ruthiraan[*,§], E. C. Abdullah[*,¶,**], N. M. Mubarak[†,‖,**] and Sabzoi Nizamuddin[‡]
[*]*Malaysia-Japan International Institute of Technology*
Universiti Teknologi Malaysia, Jalan Sultan Yahya Petra
54100 Kuala Lumpur, Malaysia
[†]*Department of Chemical Engineering*
Faculty of Engineering and Science
Curtin University, Sarawak 98009, Malaysia
[‡]*School of Engineering*
RMIT University, Melbourne 3001, Australia
[§]*ruthimaran89@gmail.com*
[¶]*ezzatc@utm.my, ezzatchan@gmail.com*
[‖]*mubarak.mujawar@curtin.edu.my, mubarak.yaseen@gmail.com*

Received 23 January 2017
Accepted 13 September 2017
Published 20 September 2018

Wastewater discharge from textile industries contribute much to water pollution and threaten the aqua ecosystem balance. Synthesis of agriculture waste based adsorbent is a smart move toward overcoming the critical environmental issues as well as a good waste management process implied. This research work describes the adsorption of methylene blue dye from aqueous solution on nickel oxide attached magnetic biochar derived from mangosteen peel. A series of characterization methods was employed such as FTIR, FESEM analysis and BET surface area analyzer to understand the adsorbent behavior produced at a heating temperature of 800°C for 20 min duration. The adsorbate pH value was varied to investigate the adsorption kinetic trend and the isotherm models were developed by determining the equilibrium adsorption capacity at varied adsorbate initial concentration. Equilibrium adsorption isotherm models were measured for single component system and the calculated data were analyzed by using Langmuir, Freundlich, Tempkin and Dubinin–Radushkevich isotherm equations. The Langmuir, Freundlich and Tempkin isotherm model exhibit a promising R^2-correlation value of more than 0.95 for all three isotherm models. The Langmuir isotherm model reflectsan equilibrium adsorption capacity of 22.883 $mg \cdot g^{-1}$.

Keywords: Magnetic biochar; methylene blue dye; mangosteen; muffle furnace; kinetic; nickel oxide.

**Corresponding authors.

1. Introduction

Technology advancement has facilitated mankind development toward hassle-free lifestyle. This virtuous effort of researchers all around the world became handicapped when it lead to various environmental issues. Accumulation of bio-waste is one of the major problem encountered by environmentalists and numerous methods have been engineered to compensate the problem arise. Converting biochar into char or solid carbon form is a common practice employed by many from the past century. During the early stage, bio-wastes were mainly pyrolyzedto use for agricultural purposes until researchers found the extraordinary trait of biochar to be further used for wastewater treatment. Activated carbon and biochar produced from discarded biomassbecame a helping hand in this area till they face limitation: low adsorption efficiency of biochar due to less surface area and two stage synthesis process of activated carbon. These factors have further driven the interest of researchers to look for substituent which is cheap in cost with high adsorption capacity and easy handling. The introduction of magnetic properties on the surface biochar has enhanced the porosity of this adsorbent which is more efficient and easy to handle for wastewater treatment at both pilot plant scale and industrial scale.[1]

Magnetism is a branch of physics that has been widely used in a much real application for ease of separation process and transportation process. The magnetic effect may be permanent or temporary. Permanent magnets, made from materials such as iron, experience the strongest effects, known as ferromagnetism.[2,3] The introduction of ferrous ions onto an organic substance create metallic effect leading to the attainment of magnetic property. Magnetic biochar is a new member in the array of carbon-based material family besides activated carbon and biochar which are widely used in various applications.[4] Magnetic Biochar is a variety of charcoal synthesized from a mixture of biomass and powdered magnetite or iron oxide that undergoes pyrolysis at different temperatures. Magnetic biochar is becoming more and more attractive to the scientific community because of its multifunctional nature. It is environment-friendly with significant uses in agriculture. It can be used in decreasing the concentration of greenhouse gases in the air, carbon storage and adsorption of both metallic toxins and organic pollutants from wastewater. Magnetic biochar is used for the removal of heavy metal ions. This property relies on the interaction between compounds with specific functional groups found on the absorbent surface. The functional groups are the factors that determine the capacity, selectivity, effectiveness and re-use of the absorbent.

Wastewater treatment process is a challenging task for Environmental Engineers as various pollutant molecules and ions bind together with water molecules which much contribute to water pollution. Numerous chemical industries such as metal, textile, fertilizers and many other industries release various types of heavy metals such as zinc, cadmium,[5] chromium[6] and nickel.[7] The presence of these types of contaminants in wastewater lead to serious threats to human beings affecting the central nervous system,[8] increased chances of lung cancer,[9] mental retardation, gastrointestinal disorder, abdominal pain[10] and a range of other diseases. Heavy metal disrupts the food chain and causes risk to the entire ecosystem and living resources. These impurities must be removed from wastewaters before discharge as they are considered importunate,[11] bio-accumulative and toxic substances. Adsorption is considered as one of the most effective studies due to its feasibility of escalating from lab study to industrial scale as reported by other researchers. Besides the role of chemical reactivity in enhancing adsorption process, some operating parameters alteration lead to the development of some mathematical tools to increase the adsorption capacity. Adsorption isotherms and kinetics studies were developed to measure the sorption capability of various types of adsorbents. These models help to further understand the adsorption behavior of different types of adsorbent and adsorbate.

Through kinetic study, the solute uptake rate can be established which determines the residence time needed for completion of adsorption reaction. Adsorption kinetics is the basic study to determine the performance of all kinds of flow-through systems such as fixed-bed. In the past decades, many mathematical models have been proposed to analyze adsorption data efficiently. These models are generally classified as adsorption reaction models and adsorption diffusion models. An evergreen problem in kinetic studies is the variation of reactant concentration over time as the reaction proceeds. Therefore, to measure the rate of change of one reactant independent of the rate of change of another reactant, requires clever experimental

design. Lagergren[12] gave a first-order equation to describe the process of adsorption of oxalic acid and malonic acid onto charcoal at the liquid-solid phase. This model is believed to be the earliest model expressing the rate of adsorption in terms of adsorption capacity. Pseudo-first-order equation is one of the measuring formulaeto distinguish the kinetic behavior based on adsorption capacity from equations based on solution concentration.[13] This equation has been frequently used to describe the adsorption of contaminants present in wastewater in different fields. Some of such instances are the adsorption of methylene blue from aqueous solution by broad bean peels and the removal of malachite green from aqueous solutions using oil palm trunk fiber.[14,15] In a study done by Ho in 1998, he described the kinetics of the process of adsorption of divalent metal ions onto peat.[13,16] The study focuses on the chemical bonding between divalent metal ions and polar functional groups present on peat, such as aldehydes, ketones, phenolics and acids that are responsible for the cation-exchange capacity of peat.[17] Ho's second-order rate equation is called pseudo-second-order rate equation to distinguish the equation from kinetic rate equations based on the concentration of the solution.[18] This equation can be effectively applied to the adsorption of dyes, metal ions, herbicides and organic substances and oils from aqueous solutions.

This study aimed to study the adsorption kinetics and isotherm models of methylene blue dye onto the surface of mangosteen peel derived magnetic biochar. The synthesis of magnetic biochar took place by impregnating nickel oxide ions onto raw biomass prior to pyrolyze in modified electric furnace at zero oxygen condition. The single system batch mode adsorption study was carried out by manipulating the operating parameters such as pH and adsorbate initial concentration. The surface morphology and structural properties of the produced magnetic biochar were characterized and the optimized magnetic biochar was used for methylene blue dye.

2. Material and Methodology

2.1. *Raw material*

All chemicals used in this study are of analytical grade quality purchased from Friendemann Schmidt and used as received. The Mangosteen peels were collected locally in Penang and were thoroughly washed to remove impurities and fungus.

2.2. *Synthesis of magnetic biochar*

In this study, we prepared NiO attached biomass by drying ground and sieved raw biomass with 1.0 M NiO into 1 L beaker and well stirred until uniformity of the suspension is reached. Then, the mixture was sonicated for 5 h at 40°C with 70% sonicating frequency (model: Elmasonic) by adding 0.4 M of $KMnO_4$ and HNO_3 aqueous solution at a ratio of 1:3. The suspension was further dried till minimal moisture content was obtained.

The second stage process involves the synthesis of nickel oxide magnetic biochar, MBN. The production of MBN was carried out in a modified Muffle Furnace model WiseTherm, FP-03, 1000°C, 3 L at zero oxygen environment. 50 g of well-dried mixture was filled in a crucible and the furnace door was closed tightly. The suction pump was connected at the top valve of the furnace to achieve zero oxygen content. The suction was continued until the suction pressure is stabilized which indicates that all the air particles inside the furnace was removed and the valve was tight prior to pyrolysis process. The pyrolysis process was conducted at 800°C for 20 min. After being cooled to room temperature, the produced MBN was washed repeatedly with deionized water to remove impurities and to achieve pH 7.0.

2.3. *Characterization of magnetic biochar*

The surface morphology and traits of MBN synthesized at optimum conditions were analyzed by opting various characterization studies. The surface structure and metal ion binding were determined using Field-emission scanning electron microscopy (FESEM) (Brand: Zeiss Model: Auriga). The presence of various functional groups on the surface of the adsorbent due to the introduction of HNO_3 and $KMnO_4$ aqueous solutions and these solutions believe to be surface pores enhancer. The functional groups formed on the surface of MBN as the product of pyrolysis was analyzed by using the Fourier Transform Infrared (FTIR) (Brand: Bruker, Model: IFS66v/S) spectroscope. Autosorb 1 surface area analyzer was used in this study to analyze the BET surface area of the adsorbent by using nitrogen adsorption at 77 K and drying of the sample at 200°C for 10 h.

2.4. *Adsorption isotherm model*

To explore novel adsorbents and establish an ideal adsorption system, it is essential to determine the most appropriate adsorption equilibrium correlation, which is indispensable for reliable prediction of adsorption parameters and quantitative comparison of adsorbent behavior for different adsorbent systems. Equilibrium relationships between a number of adsorbed particles and time at constant temperature, commonly known as adsorption isotherms, describe the interaction between pollutants and the adsorbent material. This analysis is critical for optimization of the design of adsorption system, adsorption mechanism pathways, surface properties and ability to adsorb for adsorbents.

2.5. *Langmuir isotherm*

Langmuir adsorption isotherm originally developed to describe gas–solid-phase adsorption onto activated carbon, has traditionally been used to quantify and contrast the performances of different bio-sorbents.[19] This empirical model assumes monolayer adsorption that is the adsorbed layer is one molecule in thickness. The active sites for adsorption are assumed to occur at a fixed number of definitely localized sites and are identical and equivalent.[20] There is no steric hindrance and lateral interaction between the adsorbed molecules. In its derivation, Langmuir isotherm refers to homogeneous adsorption in which each molecule possess fixed enthalpy and activation energy, with no possibility of transmigration of the adsorbate in the plane of the surface. This isotherm model was originally derived for adsorption of gases on plane surface and further expanded its application for heavy metal adsorption onto soil. The Langmuir has the form as shown in Eq. (1) and the linearized form has exhibit in Eq. (2) as shown below[21]:

$$q_e = \frac{q_m K_L C_e}{1 + K_L C_e}, \tag{1}$$

$$\frac{C_e}{q_e} = \frac{1}{K_L q_m} + \frac{C_e}{q_m}, \tag{2}$$

where C_e (mgL^{-1}) is the unabsorbed adsorbate concentration, $q_e(\mathrm{mgg}^{-1})$ is the equilibrium concentration of the adsorbate after adsorption, $K_L(\mathrm{Lmg}^{-1})$ is the equilibrium constant or Langmuir constant related to the affinity of binding sites and $q_m(\mathrm{mgg}^{-1})$ represents a particle limiting adsorption capacity.

2.6. *Freundlich isotherm*

Freundlich isotherm is widely applied in heterogeneous systems especially for organic compounds or highly interactive species on activated carbon and molecular sieves. The slope ranging between 0 and 1 is a measure of adsorption intensity or surface heterogeneity, becoming more heterogeneous as its value gets closer to zero. Whereas, a value below unity implies chemisorption process where $1/n$ above 1 is an indicative of cooperative adsorption. Recently, Freundlich isotherm is criticized for its limitation of lacking a fundamental thermodynamic basis, not approaching the Henry's law at vanishing concentrations. Moreover, the Freundlich isotherm model was designed based on the assumption of exponentially decaying adsorption site energy distribution and is suitable for heterogeneous surface energy adsorption application. The computation of this isotherm model exhibit in Eq. (3) and the linearized form shown in Eq. (4) as follows:

$$q_e = K_F C_e^n, \tag{3}$$

$$\ln q_e = \frac{\ln C_e}{n} + \ln K_F, \tag{4}$$

where K_F is a Freundlich constant that shows the adsorption capacity of the adsorbent and n is a constant, which shows the greatness of the relationship between the adsorbate and adsorbent.

2.7. *Tempkin isotherm*

Tempkin equation is excellent for predicting the gas phase equilibrium (when the organization in a tightly packed structure when identical orientation is not necessary), conversely complex adsorption systems including the liquid-phase adsorption isotherms are usually not appropriate to be represented. The indirect interaction of adsorbate or adsorbent can be determined using this adsorption model. Moreover, Tempkin and Pyzhev[22] denoted that the adsorption heat decreases linearly with the sorbent surface. Tempkin isotherm has been used as shown in Eq. (5) and the linearized form shown in Eqs. (6) and (7) as follows:

$$q_e = \frac{RT}{b}(\ln AC_e), \tag{5}$$

$$q_e = B \ln A + B \ln C_e, \tag{6}$$

$$B = \frac{RT}{b}, \tag{7}$$

where, A (Lg^{-1}) is the Tempkin isotherm equilibrium binding constant, b ($\mathrm{J \cdot mol^{-1}}$) is the Tempkin isotherm constant, R is the universal gas constant ($8.314\,\mathrm{J \cdot mol^{-1} \cdot K^{-1}}$), T(K) is the temperature and B refers to heat of sorption constant.

2.8. *Dubinin–Radushkevich isotherm*

Dubinin–Radushkevich isotherm model that exhibits one of the unique features is a temperature-dependent model, which when adsorption data at different temperatures are plotted as a function of the logarithm of amount adsorbed versus the square of potential energy, all suitable data will lie on the same curve, named as the characteristic curve. The Dubinin–Radushkevich has been expressed in Eqs. (8) and (9), the adsorption free energy has expressed in Eq. (10) and the linearized form has expressed in Eq. (11) as shown below:

$$q_e = (q_m) \exp(-K_D \varepsilon^2), \tag{8}$$

$$\varepsilon = RT \ln\left(1 + \frac{1}{C_e}\right), \tag{9}$$

$$E = \frac{1}{\sqrt{2B_D}}, \tag{10}$$

$$\ln(q_e) = \ln(q_m) - K_D \varepsilon^2, \tag{11}$$

where, K_D denotes the Dubinin–Radushkevich isotherm constant ($\mathrm{mol^2 \cdot kJ^{-2}}$), ε is the dimensionless Dubinin–Radushkevich isotherm constant and B_D is the isotherm constant.

2.9. *Adsorption kinetic study of magnetic biochar*

The determination of adsorption equilibrium of methylene blue dye onto MBN was identified by performing the kinetic study. The best optimizing conditions were identified through the batch adsorption process. The optimum conditions of agitation speed and contact time were determined and the pH value was varied to perform the kinetic study. The kinetics study was done by agitating 0.3 g of adsorbent into 100 mL of $100\,\mathrm{mg \cdot L^{-1}}$ concentrated methylene blue aqueous solution. The adsorbate sample was collected during the first 5 h of the experiment with 20 min interval. The collected samples were filtered and tested using UV-Vis Spectrophotometry to analyze the optimum time reached to give maximum removal percentage of methylene blue dye. The experiment was continued for 24 h and the final concentration of the solution after 24 h was recorded. The obtained final concentration of methylene blue dye was used to calculate q_t values and a graph of q_t versus time t was plotted. The formula to calculate the q_t value is shown in Eq. (12) as follows:

$$q_t = (C_0 - C_t) \times \frac{V}{m}, \tag{12}$$

where C_0 is the initial concentration, C_t is the concentration of the solution at a respective time, m is the dosage of adsorbent used and the v represents the volume of aqueous solution. q_t was obtained in terms of mg/g.

2.10. *Adsorption isotherm study*

The adsorption behavior was studied by conducting isotherm experiments to determine the best model suitable for adsorption of methylene blue molecules onto MBN. The batch adsorption study was carried out by contacting 0.3 g of the adsorbent with 100 mL of six different initial concentrations of the blue dye which were 50, 75, 100, 125, 150 and $1000\,\mathrm{mg \cdot L^{-1}}$ into 250 mL Erlenmeyer flask. For each model studied, an independent graph was plotted to analyze the suitability of each model for adsorption. The equilibrium concentration of adsorbate ($\mathrm{mg \cdot L^{-1}}$), C_e was measured to calculate the equilibrium amount of adsorbate particles adsorbed per gram of adsorbent ($\mathrm{mg \cdot g^{-1}}$) by employing Eq. (13) below:

$$q_e = (C_0 - C_e) \times \frac{V}{m}, \tag{13}$$

where C_0 is the initial concentration of the stock solution, v is the solution volume and m is the mass of the adsorbent used in the experiment.

3. Results and Discussion

3.1. *Effect of pyrolysis time and temperature on removal of methylene blue dye*

Figure 1 represents the removal percentage of methylene blue dye by magnetic biochar produced at a vast range of time and temperature which is used to determine the optimized heating time and temperature. Figure 1, as the heating time increases from 10 min to 30 min for a constant

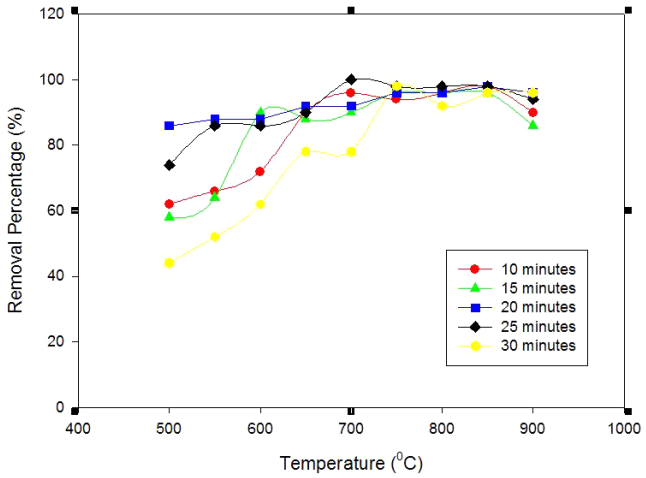

Fig. 1. Effect of pyrolysis time and temperature of nickel oxide magnetic biochar on removal of methylene blue dye.

pyrolysis temperature 700°C, the removal percentage increases. This clearly states that, longer contact time enhances the formation of surface pores and leads to increase in the surface area. The rise in heating temperature independent of time, the removal percentage for nickel oxide attached to biochar deteriorates due to destruction of surface pores which indirectly lowers down the total surface area. The rapid formation of surface pores will be destroyed as the pyrolysis process reaches a higher temperature due to continuous decomposition of surface volatile components This shows an increase in the adsorption capacity of methylene blue dye and this is due to the split in the concentration gradient between solute concentration in the solution and the solute concentration on the surface of the adsorbent.[23] Thus, decreasing in noncarbon atoms of the biomass has caused an increasing amount of formation of functional group. This may be attributed to increasing the adsorbent surface area and availability of more adsorption sites resulting from the increasing absorbent dosage. At higher absorbent to oxide concentration ratios, there is a very fast adsorption onto the surface which produces lower solute concentration in the solution.[24]

3.2. *Characterization of MBN*

Figures 2(a) and 2(b) exhibiting the FESEM images of MBN at different magnification scales were investigated to further understand the surface morphology of the nickel ions attached to the adsorbent. The formation of wide pore size distribution, from narrow microspores to wide mesopores, the removal of the exterior of the particle is significant at high burn offs. The enhancement of surface pores from raw biomass to magnetic biochar as reported by Ruthiraan *et al.*[21] and Mubarak *et al.*[25] in their previous work plays an important role in enhancing the liquid–solid adsorption processes. The formations of pores occur due to chemical decomposition of water and other organic substances which pull down the synthesis yield.[26] The introduction of oxidizing solutions such as HNO_3 and $KMnO_4$ ease the conversion of amorphous cellulose and also improves the fiber surface adhesive characteristics by removing natural and artificial impurities and produced a rough surface.[27] As reported by Mubarak *et al.* in his work that magnetic biochar exhibit larger cavities and rough surface compared to raw biomass. These behaviors are more pronounced as the heating time and temperature are varied.[28]

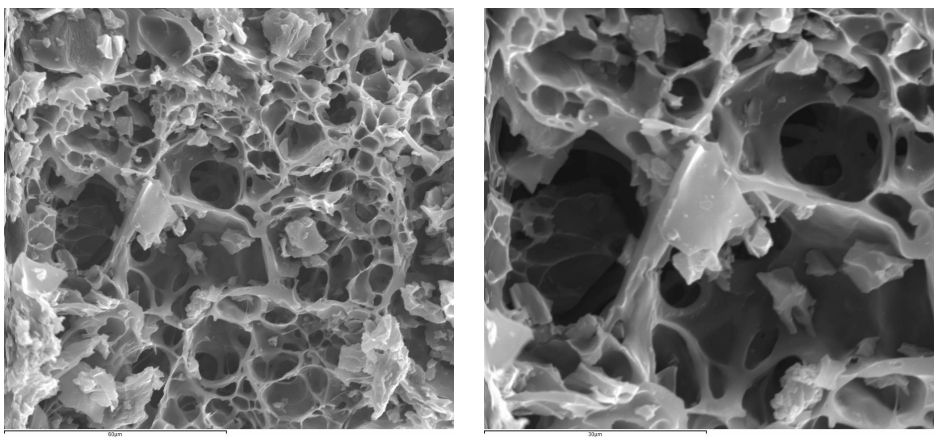

(a) (b)

Fig. 2. FESEM image of MBN (a) 1000× 20 kV and (b) 2000× 20 kV.

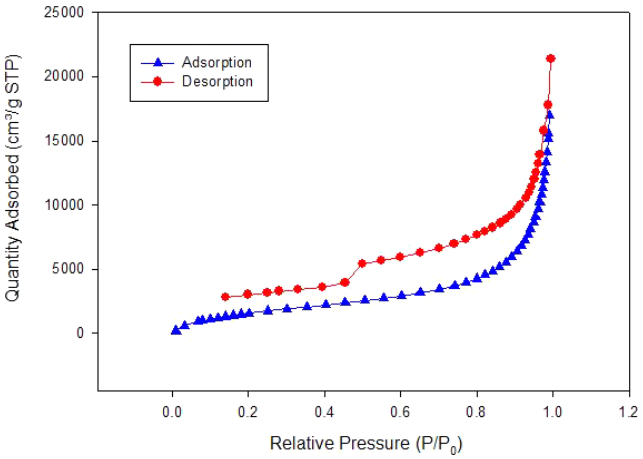

Fig. 3. N_2 adsorption/desorption at 77 K of MBN.

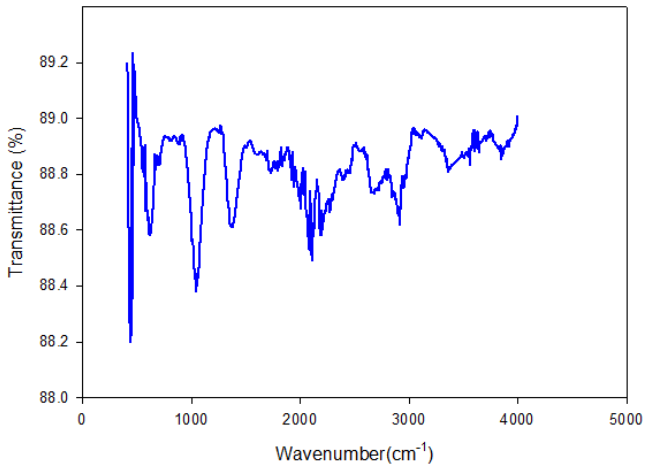

Fig. 4. FTIR spectra of MBN.

The nitrogen gas adsorption–desorption isotherm at 77 K of MBN is shown in Fig. 3. The isotherm plot type I and IV Brunauer, Deming and Teller plots which indicated the formation of micropores with exposed surface. The presence of a high ratio of micropores compared to mesopores can be identified by type I adsorption isotherm model.[29] The impregnation of raw biomas with 1.0 M nickel oxide aqueous solution in contributing for formation and widening of more surface pores which affect the increase in BET surface area. The highest BET surface area obtained at 800°C heating temperature and pyrolysis time of 20 min was $819\,m^2 \cdot g^{-1}$. Mangosteen peel is high cellulosic material, the interaction of HNO_3 and $KMnO_4$ in a vacuum environment allow the O^- atoms to bind with both aqueous solutions to decompose the volatile material at a maximum range. Besides that, the development of pore size is directly proportional to increase in BET surface area inspite of the presence metal ions on the surface of magnetic biochar. Moreover, the development of surface poresthat escalates the total BET surface area at optimum operating parameter of MBN could be due to the reactive or light-burned of metal oxide resulting from pyrolysis process at optimum conditions.[30] The total pore volume evaluated using N_2 adsorption isotherms was $0.137\,cm^3 \cdot g^{-1}$. Therefore, the presence of nickel oxide was proved to be an effective activating agent for the production of high-surface area magnetic biochar.

Figure 4 exhibiting the FTIR analysis was performed on MBN to determine the surface functional groups present on the adsorbent surface. This analysis displayed numerous peaks at wavelengths between 410 cm^{-1} to 3950 cm^{-1}. The decomposition of surface volatile substances and the effect of sonication enhance the formation of more surface functional groups. A range of broad peaks can be observed as illustrated in Fig. 4, where the peak ranging at 410–440 cm^{-1} is assigned to attachment of nickel oxide (Ni-O) on the surface of the magnetic biochar produced.[31,32] The other broad peaks represent respective functional groups: C–O–C (1000 cm^{-1}), CH_2 (2900 cm^{-1}, 1450 cm^{-1}), ester C=O (1680 cm^{-1}), 2400 cm^{-1} and –OH (3400 cm^{-1}).[33] Moreover, the presence of metal particles on the surface of biochar shifts the peaks and this explains that functional groups presented on MBN participate in complexation with metal particles.[32] Hence, the above FTIR analysis spectrum shows the disappearance of acidic functional groups with an increase in pyrolysis temperature. The magnetic biochar produced at higher temperatures are relatively alkaline in nature. The decomposition of the adsorbent surface as the effect of pyrolysis process together with the introduction of HNO_3 and $KMnO_4$ aqueous solution promote the formation of various chemical bonds on the surface. The summary of each peak shown in Table 1.

3.3. *Adsorption isotherm model study*

Adsorption isotherm is an important mathematical evaluation methodology in describing the phenomenon governing the retaining or the flowing of subtracting from an aqueous solution to a solid-phase at fixed pH and temperature.[34,35] The establishment of adsorption equilibrium time when an adsorbate containing phase has been contacted with the adsorbent can be investigated via adsorption isotherm study by determining the computational

Table 1. Summary of FTIR result MBN.

MBN band position (cm^{-1})	Possible assignments	Reference
3586–3385	O–H stretching, free hydroxyl	51
2920	C–H stretching (carboxyl)	—
2677	H–C=O: C–H stretching (aldehydes)	—
2210–2103	–C≡C– stretching (alkynes)	
1755	C=O stretching (carboxylic acids)	52
1036	C–N stretching (aliphatic amines)	53
662	=C–H bending (alkenes)	54
612	–C≡C–H:C–H bend (alkynes)	

correlation obtained from a graphical expression which contributes much toward modeling analysis, operational design and applicable practices of adsorption system.[36–38] In this study, four different isotherm models were analyzed to further understand adsorption behavior namely the Langmuir isotherm, Freundlich isotherm, Tempkin and Dubinin–Radushkevich isotherm for adsorption of methylene blue dye on MBN. The computed values were plotted using the graphical method and have been successfully illustrated in Figs. 5(a)–5(d). The formation of monolayer adsorbate on the adsorbent surface was investigated by plotting Langmuir adsorption isotherm graph as shown in Fig. 5(a). The R^2 correlation value of more than 0.95 justifies that the batch adsorption has reached the saturation point and no any further adsorption could take place. Furthermore, upon attaining adsorption equilibrium, the sorption mechanism has taken place at homogeneous sites within the adsorbent.[39] The calculated Langmuir values were presented in Table 1 where the maximum adsorption equilibrium, q_m was 22.88 $mg \cdot g^{-1}$ as reported. The greater K_L value for adsorption of methylene blue dye obtained indicates that MBN surface had a higher affinity for this organic dye molecule computation of higher maximum adsorption capacity obtained, which may due to the formation of a larger amount of surface functional groups which enhance the single layer adsorption process. The Freundlich

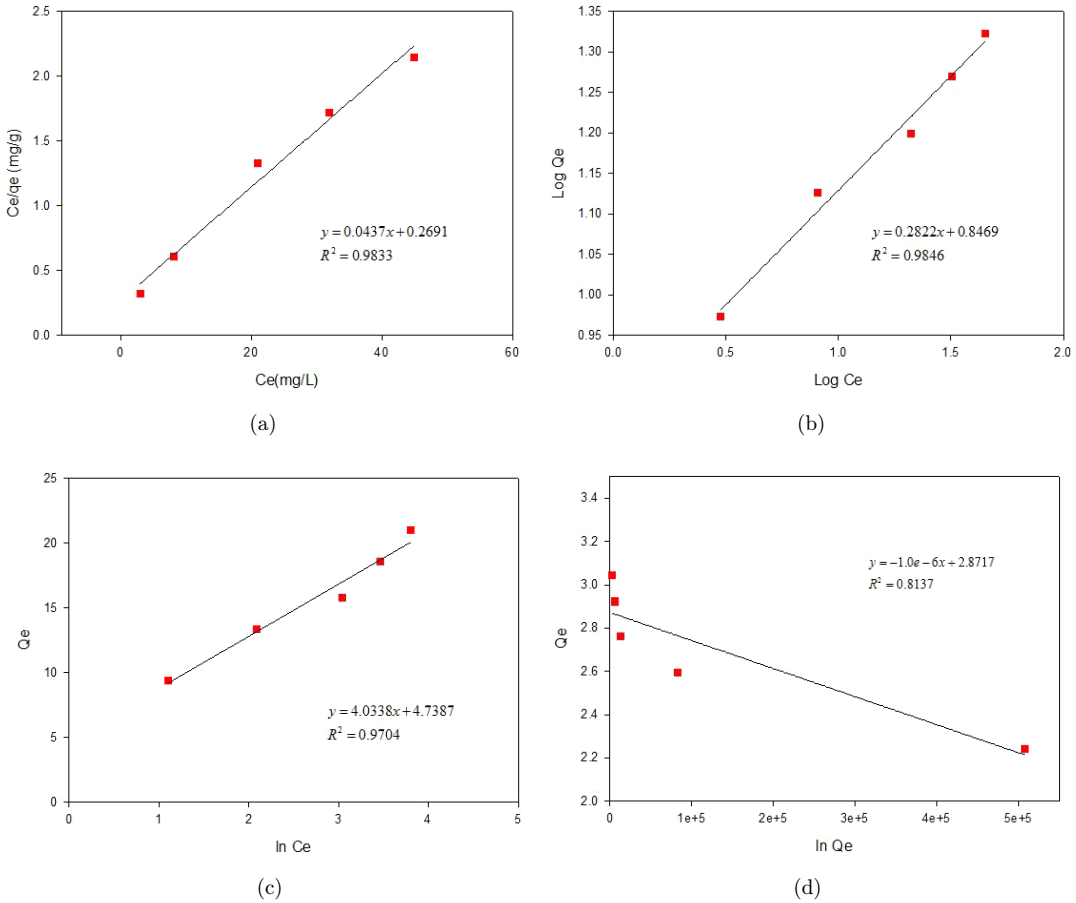

Fig. 5. (a) Langmuir isotherm, (b) Freundlich isotherm, (c) Tempkin isotherm and (d) Dubinin–Radushkevich isotherm plots for adsorption of Methylene Blue dye on MBN.

Table 2. Isotherm parameters for adsorption methylene blue dye by MBN.

Isotherm models	Parameters	MBN
Langmuir Isotherm	q_m $(\mathrm{mg \cdot g^{-1}})$	22.883
	K_L $(\mathrm{L \cdot mg^{-1}})$	0.162
	R^2	0.983
Freundlich Isotherm	K_F $(\mathrm{L \cdot g^{-1}})$	2.332
	$1/n$	0.282
	R^2	0.985
Tempkin Isotherm	A $(\mathrm{L \cdot g^{-1}})$	3.237
	B $(\mathrm{kJ \cdot mol^{-1}})$	4.034
	R^2	0.970
Dubinin–Radushkevich	q_m $(\mathrm{mg \cdot g^{-1}})$	17.667
	K $\times 10^{-7}$ $(\mathrm{mol^2 \cdot kJ^{-2}})$	10
	E $(\mathrm{kJ \cdot mol^{-1}})$	0.220
	R^2	0.814

isotherm model describes the heterogeneous surface adsorption where this equation agrees well with Langmuir over moderate concentration range but, unlike the Langmuir expression, it does not reduce to the linear isotherm (Henry_s Law) at low surface coverage.[40] The Freundlich constant $1/n$ below 1 indicates normal adsorption as shown in Table 2. The function has an asymptotic maximum as pressure increases without bound.[41] Moreover, the higher the value of $1/n$, the greater the expected heterogeneity. On the other hand, the n value between 1 and 10 explains that this isotherm model is favorable. From the data in Table 1, the R^2 correlation value of 0.985 explains that the sorption of methylene blue dye is favorable and a well-fit adsorption model.[42] The adsorbent–adsorbate interaction was well described by the Tempkin isotherm model. The well fit Tempkin adsorption isotherm explains that theadsorbate heat of adsorption present on the layer decreases linearlywith the coverage which is due to adsorbent–adsorbate interactions. On the other hand, the maximum binding energy attained during a uniform distribution of binding energy explains the adsorption characteristic.[22,43] From the Tempkin plot in Fig. 5(c), the R^2 correlation value of 0.970 obtained has explained that it is a physical adsorption. The nature of adsorption can be determined by employing the Dubinin–Radushkevich isotherm adsorption model whereas the adsorption mechanism is well expressed with Gaussian energy distribution onto a heterogeneous surface.[44] The higher R^2 correlation value usually correlates with high solute activities and the intermediate range of concentration data.[45] The computed value of mean free energy, E value describes the adsorption mechanism of the adsorbent. The value ranging between $8\,\mathrm{kJ \cdot mol^{-1}}$ and $16\,\mathrm{kJ \cdot mol^{-1}}$ denote that it favors chemical adsorption while the E value lesser than $8\,\mathrm{kJ \cdot mol^{-1}}$ explains that adsorption occurs physically. The plot of Q_e versus ln Q_e exhibit least favorable R^2 correlation value of 0.814 for adsorption of methylene blue dye on MBN.

3.4. *Adsorption kinetic study*

Adsorption is one of the most prominent and versatile technique in wastewater treatment process. The correlation between the linearity of both solute and adsorbent can be further explained using the adsorption kinetic model study. Different solutes possesses their own oxidation levels which differs according to different adsorbents in the solute separation process. This chemical behavior can be further understood by employing this mathematical method. The kinetic study does not only help to

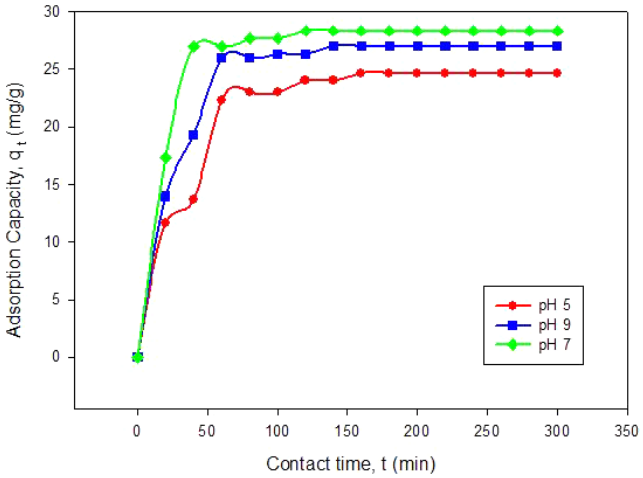

Fig. 6. Adsorption capacity (qt) versus contact time (t) with different pH of Methylene Blue dye on MBN.

Table 3. Pseudo second order of methylene blue dye by MBN.

	MBN		
pH	q_e $(\mathrm{mg \cdot g^{-1}})$	K_2 $(\mathrm{min \cdot g \cdot mg^{-1}})$	R^2
5.0	8.251	69.134	0.985
7.0	8.606	74.366	0.996
9.0	8.953	80.454	0.996

Table 4. Literature review on isotherm parameter for adsorption of methylene blue dye.

Adsorbent	q_m ($mg \cdot g^{-1}$)	K_L ($L \cdot mg^{-1}$)	R^2	K_F ($L \cdot g^{-1}$)	$1/n$	R^2	A ($L \cdot g^{-1}$)	B ($kJ \cdot mol^{-1}$)	R^2	Reference
MBN	22.883	0.162	0.983	2.323	0.282	0.985	3.237	4.034	0.970	This study
Magnetic corncob-derived adsorbent	163.93	0.216	0.999	28.199	0.223	0.893	—	—	—	55
Magnetic $Ni_{0.5}Zn_{0.5}Fe_2O_4$ nanoparticles	54.719	0.741	0.858	25.456	0.229	0.989	19.178	8.548	0.991	56
Posidoniaoceanica activated carbon	217.39	1.7	0.990	112.12	0.365	0.918	—	—	—	29
Magnetic iron oxide nanosorbent	25.54	1.39	0.999	16.48	0.115	0.824	—	—	—	57
CMCD–MNP(P)	138.9	1.028	0.998	0.121	0.337	0.957				58
CMCD–MNP(C)	77.5	0.860	0.996	0.066	0.352	0.945				58

understand the adsorption behavior but also for pilot modeling as well.[46] The plots in Fig. 6 explain the equilibrium achieved via kinetic study for adsorption of methylene blue dye on MBN. The relationship between the adsorption capacity (q_t) over time taken for fruitful adsorption were studied at different adsorbate pH. The kinetic study was conducted at three different adsorbate media namely, acidic, neutral and alkaline medium to determine the availability of the active site on the adsorbent to cooperate along with solute at different ionic strengths. A steep adsorption gradient was observed at the first 40 min. The solute uptake from the aqueous solution onto both metal ions attached biochar were plotted. As can be observed from Fig. 5, the adsorption of methylene blue dye attained equilibrium at 110 min and this adsorbent exhibited a greater adsorption capacity at any pH which has been proved via this kinetic study, but highest equilibrium adsorption, q_e, of $27.5\,mg \cdot g^{-1}$ was recorded at neutral pH. This rapidsorption rate of dyes is due to the strong bond that is formed between the blue dye and the produced magnetic biochar at equilibrium adsorbate ionic charges.[47] Initially, the adsorption of adsorbate molecules was rapid and reduced with the passage of time due to the availability of the active site on the adsorbent to promote the adsorption rate and diminished gradually upon attaining equilibrium. The kinetics studies reveal that adsorption of methylene blue dye on MBN shows the independence of electrostatic interaction.

The solute adsorption behavior on adsorbent can be further understood by employing various kinetic model studies. Computation of kinetic model is very important in describing the correlation between the adsorbent and adsorbate.[48] The pseudo-second order model exhibits predominant adsorption mechanism because of the contribution of both physisorption and chemisorption for enhancement of sorption uptake of solute.[47] Moreover, many researchers have done a series of kinetic studies and it has been found that pseudo-second-order model can provide a better relationship for the kinetics of adsorption process.[43,49,50] Thepseudo-second-order methylene blue dye models were used toanalyze the adsorption kinetic as shown in the equation below:

$$\frac{t}{q_t} = \frac{1}{K_2 q_e^2} + \frac{t}{q_e}, \tag{14}$$

where, $K_2(gmol^{-1}\ min)$ is the rate constant of the pseudo-second-order adsorption, q_e and q_t are the amounts of methylene blue dye adsorbedon adsorbent (mol/g) at equilibrium and at time t, respectively. Applying the above equation, pseudo-second-order adsorption graph were plotted for $t/q_t(min \cdot g \cdot mg^{-1})$ versus time (min) as shown in Fig. 6 for MBN. The computation of the mathematical equation explains that all of the data converged well into a straight line with a high correlation with coefficient of determination (R^2) falling in the range 0.993–0.999 for the increase in pH from 5 to 9 as tabulated in Table 3. Review on methylene blue dye adsorption using magnetised carbon-based adsorbent as shown in Table 4.

4. Conclusions

This research work has shown that mangosteen peel derived magnetic biochar is an effective adsorbent for adsorption of methylene blue dye from aqueous solution. The MBN produced has higher BET surface

area of $819\,m^2 \cdot g^{-1}$. The introduction of both 0.4 M $KMnO_4$ and 0.4 M HNO_3 solutions during biomass sonication process promote the enhancement of surface pores as reflected on higher BET surface area obtained. The Langmuir, Freundlich and Tempkin isotherm models fit well to this batch adsorption study compared to Dubinin–Radushkevich isotherm model. The pseudo-second-order kinetic model resemblessimilar equilibrium adsorption capacity at all three different pH values of 5.0, 7.0 and 9.0. The highest value obtained was $8.953\,mg \cdot g^{-1}$ at pH 9.0 with the high R^2 correlation value of 0.996. The methylene blue dye removal by using MBN follows the pseudo-second-order kinetic model, which is chemisorption dependent and may be the rate-limiting step. The blue dye molecules bind with adsorbent surface functional groups by chemical bonding and utilize the surface pores to maximize their coordination number with the surface.

Acknowledgment

This work was fully supported by Malaysia-Japan International Institute of Technology under FRGS/2/2013/TK05/UTM/01/5.

References

1. D. Granatstein, C. Kruger, H. Collins, S. Galinato, M. Garcia-Perez and J. Yoder, Use of biochar from the pyrolysis of waste organic material as a soil amendment. Final project report, Center for Sustaining Agriculture and Natural Resources, Washington State University, Wenatchee, WA (2009).
2. J. B. Pendry, D. Schurig and D. R. Smith, *Science* **312**, 1780 (2006).
3. S. M. Walker, *Magnetism* (Lerner Publications, 2005).
4. J. R. Reitz, F. J. Milford and R. W. Christy, *Foundations of Electromagnetic Theory* (Addison-Wesley Publishing Company, 2008).
5. O. Yavuz, R. Guzel, F. Aydin, I. Tegin and R. Ziyadanogullari, *Polish J. Environ. Stud.* **16**, 467 (2007).
6. N. Mubarak, R. Thines, N. Sajuni, E. Abdullah, J. Sahu, P. Ganesan and N. Jayakumar, *Korean J. Chem. Eng.* **31**, 1582 (2014).
7. K. Periasamy and C. Namasivayam, *Waste Manage.* **15**, 63 (1995).
8. Y.-H. Li, S. Wang, J. Wei, X. Zhang, C. Xu, Z. Luan, D. Wu and B. Wei, *Chem. Phys. Lett.* **357**, 263 (2002).
9. J. Acharya, J. N. Sahu, C. R. Mohanty and B. C. Meikap, *Chem. Eng. J.* **149**, 249 (2009).
10. A. K. Bhattacharya, S. N. Mandal and S. K. Das, *Chem. Eng. J.* **123**, 43 (2006).
11. D. Mohan, H. Kumar, A. Sarswat, M. Alexandre-Franco and C. U. Pittman Jr, *Chem. Eng. J.* **236**, 513 (2014).
12. S. Lagergren, About the theory of so-called adsorption of soluble substances **24**, 1 (1898).
13. Y.-S. Ho and G. McKay, *Process Safety Environ. Protect.* **76**, 183 (1998).
14. B. Hameed and M. El-Khaiary, *J. Hazardous Mater.* **154**, 237 (2008).
15. B. Hameed and M. El-Khaiary, *J. Hazardous Mater.* **159**, 574 (2008).
16. Y.-S. Ho and G. McKay, *Chem. Eng. J.* **70**, 115 (1998).
17. N. Coleman, A. McClung and D. P. Moore, *Science* **123**, 330 (1956).
18. Y.-S. Ho, *J. Hazardous Mater.* **136**, 681 (2006).
19. K. Foo and B. Hameed, *Chem. Eng. J.* **156**, 2 (2010).
20. K. Vijayaraghavan, T. Padmesh, K. Palanivelu and M. Velan, *J. Hazardous Mater.* **133**, 304 (2006).
21. M. Ruthiraan, N. M. Mubarak, R. K. Thines, E. C. Abdullah, J. N. Sahu, N. S. Jayakumar and P. Ganesan, *Korean J. Chem. Eng.* **32**, 446 (2015).
22. M. Tempkin and V. Pyzhev, *Acta Phys. Chim. USSR* **12**, 327 (1940).
23. O. Hamdaoui, F. Saoudi, M. Chiha and E. Naffrechoux, *Chem. Eng. J.* **143**, 73 (2008).
24. L. Nouri, I. Ghodbane, O. Hamdaoui, M. Chiha, *J. Hazardous Mater.* **149**, 115 (2007).
25. N. M. Mubarak, R. F. Alicia, E. C. Abdullah, J. N. Sahu, A. B. A. Haslija and J. Tan, *J. Environ. Chem. Eng.* **1**, 486 (2013).
26. D. Mohan, S. Rajput, V. K. Singh, P. H. Steele and C. U. Pittman, *J. Hazardous Mater.* **188**, 319 (2011).
27. S. Song, N. Saman, K. Johari and H. Mat, *J. Teknol.* **63**, 67 (2013).
28. N. M. Mubarak, A. Kundu, J. N. Sahu, E. C. Abdullah and N. S. Jayakumar, *Biomass Bioenergy* **61**, 265 (2014).
29. M. U. Dural, L. Cavas, S. K. Papageorgiou and F. K. Katsaros, *Chem. Eng. J.* **168**, 77 (2011).
30. A. R. Usman, M. Ahmad, M. El-Mahrouky, A. Al-Omran, Y. S. Ok, A. S. Sallam, A. H. El-Naggar and M. I. Al-Wabel, *Environ. Geochemistry Health* **38**, 511 (2015).
31. A. E. Pirbazari, E. Saberikhah and S. H. Kozani, *Water Resources Industry* **7**, 23 (2014).
32. Y. Wang, X. Wang, X. Wang, M. Liu, Z. Wu, L. Yang, S. Xia and J. Zhao, *J. Ind. Eng. Chem.* **19**, 353 (2013).
33. B. Chen, Z. Chen and S. Lv, *Bioresource Technol.* **102**, 716 (2011).

34. G. Limousin, J.-P. Gaudet, L. Charlet, S. Szenknect, V. Barthes and M. Krimissa, *Appl. Geochem.* **22**, 249 (2007).
35. S. Allen, G. Mckay and J. Porter, *J. Colloid Interface Sci.* **280**, 322 (2004).
36. K. V. Kumar and S. Sivanesan, *Dyes Pigments* **72**, 130 (2007).
37. M. Ghiaci, A. Abbaspur, R. Kia and F. Seyedeyn-Azad, *Sep. Purification Technol.* **40**, 217 (2004).
38. M. C. Ncibi, *J. Hazardous Mater.* **153**, 207 (2008).
39. I. Langmuir, *J. Am. Chem. Soc.* **40**, 1361 (1918).
40. S. J. Allen, Q. Gan, R. Matthews and P. A. Johnson, *Bioresource Technol.* **88**, 143 (2003).
41. S. V. Mohan and J. Karthikeyan, *Environ. Pollut.* **97**, 183 (1997).
42. S. Goldberg, M. Tabatabai, D. Sparks, L. Al-Amoodi and W. Dick, *Chem. Processes Soils* 489 (2005).
43. H. Javadian, F. Ghorbani, H.-A. Tayebi and S. H. Asl, *Arabian J. Chem.* **8**, 837 (2013).
44. A. Günay, E. Arslankaya and I. Tosun, *J. Hazardous Mater.* **146**, 362 (2007).
45. A. Dąbrowski, *Adv. Colloid Interface Sci.* **93**, 135 (2001).
46. H. Qiu, L. Lv, B.-C. Pan, Q.-J. Zhang, W.-M. Zhang and Q.-X. Zhang, *J. Zhejiang Univ. Sci. A* **10**, 716 (2009).
47. E. Moawed and M. El-Shahat, *J. Taibah Univ. Sci.* **10**, 46 (2016).
48. M. Abbas and M. Trari, *Process Safety Environ. Protection* **98**, 424 (2015).
49. A. Bhattacharya, T. Naiya, S. Mandal and S. Das, *Chem. Eng. J.* **137**, 529 (2008).
50. L. Lian, X. Cao, Y. Wu, D. Sun and D. Lou, *Appl. Surf. Sci.* **289**, 245 (2014).
51. M. Giovanela, E. Parlanti, E. Soriano-Sierra, M. Soldi and M. Sierra, *Geochem. J.* **38**, 255 (2004).
52. J. Goel, K. Kadirvelu, C. Rajagopal and V. K. Garg, *J. Hazardous Mater.* **125**, 211 (2005).
53. M. Matias, M. De La Orden, C. G. Sánchez and J. M. Urreaga, *J. Appl. Polym. Sci.* **75**, 256 (2000).
54. F. B. Reig, J. G. Adelantado and M. M. Moreno, *Talanta* **58**, 811 (2002).
55. H. Ma, J.-B. Li, W.-W. Liu, M. Miao, B.-J. Cheng and S.-W. Zhu, *Bioresource Technol.* **190**, 13 (2015).
56. L. Ruijiang, S. Xiangqian, Y. Xinchun, W. Qiuju and Y. Fang, Adsorption characteristics of methyl blue onto magnetic $Ni_{0.5}Zn_{0.5}Fe_2O_4$ nanoparticles prepared by the rapid combustion process, Chapter 10, (2013).
57. C. Păcurariu, O. Paşka, R. Ianoş and S. G. Muntean, *Clean Technol. Environ. Policy* 1 (2015).
58. A. Badruddoza, G. S. S. Hazel, K. Hidajat and M. Uddin, *Colloids Surf. A Physicochem. Eng. Aspects* **367**, 85 (2010).